

# Modelling Water Flow and Solute Transport in Heterogeneous Unsaturated Porous Media

Gerardo Severino, Alessandro Santini, and Valeria Marina Monetti

**Abstract** New results concerning flow velocity and solute spreading in an unbounded three-dimensional partially saturated heterogeneous porous formation are derived. Assuming that the effective water content is a uniformly distributed constant, and dealing with the recent results of Severino and Santini (*Advances in Water Resources* 2005;28:964–974) on mean vertical steady flows, first-order approximation of the velocity covariance, and of the macrodispersion coefficients are calculated. Generally, the velocity covariance is expressed via two quadratures. These quadratures are further reduced after adopting specific (i.e., exponential) shape for the required (cross)correlation functions. Two particular formation structures that are relevant for the applications and lead to significant simplifications of the computational aspect are also considered.

It is shown that the rate at which the Fickian regime is approached is an intrinsic medium property, whereas the value of the macrodispersion coefficients is also influenced by the mean flow conditions as well as the (cross)-variances  $\sigma^2_\gamma$  of the input parameters. For a medium of given anisotropy structure, the velocity variances reduce as the medium becomes drier (in mean), and it increases with  $\sigma^2_\gamma$ . In order to emphasize the intrinsic nature of the velocity autocorrelation, good agreement is shown between our analytical results and the velocity autocorrelation as determined by Russo (*Water Resources Research* 1995;31:129–137) when accounting for groundwater flow normal to the formation bedding. In a similar manner, the intrinsic character of attainment of the Fickian regime is demonstrated by comparing the scaled longitudinal macrodispersion coefficients  $\frac{D_{11}(t)}{D_{11}(\infty)}$  as well as the lateral displacement variance  $\frac{X_{22}(t)}{X_{22}(\infty)} = \frac{X_{33}(t)}{X_{33}(\infty)}$  with the same quantities derived by Russo (*Water Resources Research* 1995;31:129–137) in the case of groundwater flow normal to the formation bedding.

---

G. Severino (✉)

Division of Water Resources Management, University of Naples Federico II, Naples, Italy

e-mail: severino@unina.it

## 1 Introduction

Water flow and solute transport in a heterogeneous unsaturated porous formation (hereafter also termed *vadose zone*) are determined by the inherent variability of the hydraulic formation properties (like the conductivity curve), flow variables (e.g., the flux), and boundary conditions imposed on the domain. Because the formation properties are highly variable, the resultant uncertainty of their spatial distribution is usually modelled within a stochastic framework that regards the formation property as a random space function (RSF). As a consequence, flow and transport variables become RSFs, as well.

For given statistics of the flow field, solute spreading can be quantified in terms of the first two moments of the probability density function of the solute particles displacement. This task has been accomplished by [4, 20] for transport by groundwater and unsaturated flow, respectively. However, in the case of unsaturated flow, it is much more difficult due to the nonlinearity of the governing equations. By using the stochastic theory developed in [20, 35, 36], Russo [20] derived the velocity covariance that is required to model transport in a vadose zone. Then, Russo [20] predicted the continuous transition from a convection-dominated transport applicable at small travel distances to a convection-dispersion transport valid when the solute body has covered a sufficiently large distance. Assuming that the mean flow is normal to the formation bedding, Russo [24] derived the velocity covariance tensor and the related macrodispersion coefficients showing that the rate of approaching the asymptotic (Fickian) regime is highly influenced by the statistics of the relevant formation properties. The assumption of mean flow normal to the formation bedding was relaxed in a subsequent study [25].

All the aforementioned studies were carried out by assuming that, for a given mean pressure head, the water content can be treated as a constant because the spatial variability of the retention curve is normally found very small compared with that of the conductivity curve [19, 26, 29]. More recently, Russo [27] has investigated the effect of the variability of the water content on flow and transport in a vadose zone. He has shown that the water content variability increases the velocity variance, and therefore it enhances solute spreading. Such results were subsequently refined by Harter and Zhang [10]. Further extensions of these studies were provided by Russo [28] who considered flow and transport in a bimodal vadose zone.

In this chapter, we derive new expressions for the velocity covariance. Unlike the previous approach mainly developed by [20, 23, 27] and relying on the stochastic theory of [35, 36], we make use of the recent results of [30]. Such a choice is motivated by the fact that we can obtain very simple results. Then, by adopting the Lagrangian approach developed in the past, we analyze solute spreading in a vadose zone with special emphasis on the impact of the spatial variability of the formation properties upon attainment the Fickian regime.

## 2 The General Framework

The study is carried out in two stages. In the first, we relate the statistical moments of the flux to those of the porous formation as well as mean flow conditions, and in the second, we use the previously derived statistics to analyze solute spreading .

### 2.1 Derivation of the Flux Statistics

We consider an unbounded domain of a vadose zone with statistically anisotropic structure in a Cartesian coordinate system  $x_i$  ( $i = 1, 2, 3$ ) with  $x_1$  downward oriented. In order to relate the statistical moments of the flux  $\mathbf{q}$  to those of the porous formation, the following assumptions are employed: (i) the local steady-state flow obeys the unsaturated Darcy’s law and continuity equation

$$\mathbf{q}(\mathbf{x}) = -K(\Psi, \mathbf{x})\nabla(\Psi + x_1) \quad \nabla \cdot \mathbf{q} = 0 \tag{1}$$

respectively, and (ii) the local relationship between the conductivity  $K = K(\Psi, \mathbf{x})$  and the pressure head  $\Psi$  is nonhysteretic, isotropic, and given by the model of [8]

$$K(\Psi, \mathbf{x}) = K_s(\Psi, \mathbf{x}) \exp[\alpha(\mathbf{x})\psi] \tag{2}$$

where  $\alpha$  is a soil pore-size distribution parameter, whereas  $K_s(\mathbf{x}) = K_s(0, \mathbf{x})$  represents the saturation conductivity. The range of applicability of the conductivity model (2) has been discussed by [18], and its usefulness to analyze transport has been assessed [20].

Owing to the scarcity of data, and because of their large spatial variations,  $K_s$  and  $\alpha$  are regarded as stationary RSFs defined through their log-transforms  $Y$  and  $\zeta$  as follows:

$$K_s = K_G = \exp(Y') \quad \alpha = \alpha_G \exp(\zeta') \quad K_G = \exp(\langle Y \rangle) \quad \alpha_G = \exp(\langle \zeta \rangle) \tag{3}$$

in which  $\langle \rangle$  denotes the expected value, and the prime symbol represents the fluctuation. In line with numerous field findings (e.g., [13, 17, 34, 26]), we assume that the various (cross)correlation functions  $C_\gamma(\gamma = Y, \zeta, Y\zeta)$  have axisymmetric structure, that is,

$$C_\gamma(x) = \sigma_\gamma^2 \rho_\gamma(x) \quad x = |\mathbf{x}| = \sqrt{\left(\frac{x_1}{I'_v}\right)^2 + \left(\frac{x_2}{I^\gamma}\right)^2 + \left(\frac{x_3}{I^\gamma}\right)^2} \tag{4}$$

where  $\sigma_\gamma^2$  and  $\rho_\gamma(x)$  represent the variance and the autocorrelation, respectively, whereas  $I'_v$  and  $I^\gamma$  are the vertical and horizontal integral scale of the  $\gamma$ -parameters. Whereas there is a large body of literature devoted to the spatial

variability of  $Y$  (for a wide review, see [5]), limited information on  $\zeta$  is available. However, some studies ([16, 19, 26, 33, 34]) have shown that the  $\gamma$ -RSFs exhibit very similar integral scales. Thus, based on these grounds, we shall assume that  $I'_v \equiv I_v$ ,  $I^\lambda \equiv I$  and  $\rho_\gamma(x) \equiv \rho(x)$ . Furthermore, we shall consider hereafter a flow normal to the formation bedding that represents the most usual configuration encountered in the applications ([9, 37]).

By dealing with the same flow conditions (i.e., mean vertical steady flow in an unbounded vadose zone) considered by [30], the first-order fluctuation  $\mathbf{q}'$  is given by (see second of Equation (8) in [30]):

$$\mathbf{q}'(\mathbf{x}) = -\exp(\langle\Psi\rangle)[Y'(\mathbf{x}) + \Psi_1(\mathbf{x}) + \langle\Psi\rangle\zeta'(\mathbf{x})]\mathbf{e}_1 + \nabla\Psi_1(\mathbf{x}) \quad (5)$$

(where  $\mathbf{e}_1$  is the vertical unit vector). Let us observe that the fluctuation (5) has been rewritten after scaling the lengths by  $\alpha_G^{-1}$  and the velocities by  $K_G$  (although for simplicity we have retained the same notation). Then, by using the spectral representation of the quantities appearing on the right-hand side of (5) leads to

$$q_1'(\mathbf{x}) = -\exp(\langle\Psi\rangle) \int \frac{d\mathbf{k}}{(2\pi)^{3/2}} \exp(-j\mathbf{k} \cdot \mathbf{x}) [\tilde{Y}'(\mathbf{k}) + \langle\Psi\rangle\tilde{\zeta}'(\mathbf{k})] \frac{k^2 - k_1^2}{k^2 + jk_1} \quad (6a)$$

$$q_m'(\mathbf{x}) = -\exp(\langle\Psi\rangle) \int \frac{d\mathbf{k}}{(2\pi)^{3/2}} \exp(-j\mathbf{k} \cdot \mathbf{x}) [\tilde{Y}'(\mathbf{k}) + \langle\Psi\rangle\tilde{\zeta}'(\mathbf{k})] \frac{k_1 k m}{k^2 + jk_1} \quad (6b)$$

with  $\tilde{f}(\mathbf{k}) = \int \frac{d\mathbf{x}}{(2\pi)^{3/2}} \exp(j\mathbf{k} \cdot \mathbf{x}) f(\mathbf{x})$  being the Fourier transform of  $f(\mathbf{x})$  (hereafter  $m = 2, 3$ ). The flux covariance  $C_{q_i}$  (we assume that the coordinate axes are principal) is obtained by averaging the product  $q_i'(\mathbf{x})q_i'(\mathbf{y})$ , that is,

$$C_{q_i}(\mathbf{r}) = \sigma^2 \exp(2\langle\Psi\rangle)\chi_i(\mathbf{r}) \quad (7)$$

with  $\sigma^2 = \sigma_Y^2 + 2\langle\Psi\rangle\sigma_{Y\zeta} + (\langle\Psi\rangle\sigma_\zeta)^2$ . Because of the linear dependence of the fluctuation  $\mathbf{q}'$  upon the Fourier transform of  $Y$  and  $\zeta$  [see Equations (6a)–(6b)], the covariance (7) depends only upon the separation distance  $\mathbf{r} = \mathbf{x} - \mathbf{y}$  between two arbitrary points  $\mathbf{x}$  and  $\mathbf{y}$  belonging to the flow domain. The functions  $\chi_i$  needed to evaluate (7) are defined as

$$\chi_i(\mathbf{r}) = \begin{cases} \int \frac{d\mathbf{k}}{(2\pi)^{3/2}} \exp(-j\mathbf{k} \cdot \mathbf{r}) \tilde{\rho}(\mathbf{k}) \frac{(k^2 - k_1^2)^2}{k^4 + k_1^2} & i = 1 \\ \int \frac{d\mathbf{k}}{(2\pi)^{3/2}} \exp(-j\mathbf{k} \cdot \mathbf{r}) \tilde{\rho}(\mathbf{k}) \frac{(k_1 k i)^2}{k^4 + k_1^2} & i = m \end{cases} \quad (8)$$

and they quantify the impact of the medium heterogeneity structure on the flux covariance. Before dealing with the most general case, we want to consider here

two particular anisotropic heterogeneity structures that enable one to simplify the computational effort and are at the same time relevant for the applications.

The first pertains to highly vertically anisotropic formations. It applies to those soils where the parameters can be considered correlated over very short vertical distances. The assumption of high vertically anisotropic formations is quite reasonable for sedimentary soils for which it has been shown that the rate of decay of the hydraulic properties correlation in the vertical direction is very rapid, and the integral scale in that direction may be much smaller than the integral scale in the horizontal direction (e.g., [1, 13, 17]). From a mathematical point of view, this implies that  $\gamma(x_1 + r_v)$  and  $\gamma(x_1)$  can be considered uncorrelated no matter how small is the vertical separation distance  $r_v$ . This type of approximation was already adopted by [7, 11] to investigate one-dimensional flow in partially saturated bounded formations and well-type flow, respectively. Thus, by employing such an assumption, the  $\chi_i$  functions (8) can be written as

$$\chi_i(\mathbf{r}) = \begin{cases} \frac{S_0}{2\pi^2} \int d\mathbf{k}_h \exp(-j\mathbf{k}_h \cdot \mathbf{r}_h) \tilde{\rho}(k_h) k_h^4 \int_0^\infty \frac{du \cos(r_v u)}{(u^2 + k_h^2)^2 + u^2} & i = 1 \\ \frac{S_0}{2\pi^2} \int d\mathbf{k}_h \exp(-j\mathbf{k}_h \cdot \mathbf{r}_h) \tilde{\rho}(k_h) k_i^2 \int_0^\infty \frac{du u^2 \cos(r_v u)}{(u^2 + k_h^2)^2 + u^2} & i = m \end{cases} \quad (9)$$

where the parameter  $S_0$  depends only upon the shape of  $\rho(r)$  (see, e.g., [38]), whereas  $r_h$  is the horizontal separation distance.

The integrals over  $u$  are evaluated by the residual theory yielding

$$\int_0^\infty \frac{du \cos(r_v u)}{(u^2 + k_h^2)^2 + u^2} = \frac{\pi}{2} \left[ \Theta\left(\frac{\rho_-}{2}\right) - \Theta\left(\frac{\rho_+}{2}\right) \right] (1 + 4k_h^2)^{-1/2} \quad (10a)$$

$$\int_0^\infty \frac{du u^2 \cos(r_v u)}{(u^2 + k_h^2)^2 + u^2} = \frac{\pi}{2} \left[ \frac{\rho_+}{2} \Theta\left(\frac{\rho_+}{2}\right) - \frac{\rho_-}{2} \Theta\left(\frac{\rho_-}{2}\right) \right] (1 + 4k_h^2)^{-1/2} \quad (10b)$$

$$\Theta(a) = \frac{\exp(-|r_v| \sqrt{a})}{\sqrt{a}} \quad \rho_\pm = 1 + 2k_h^2 \pm (1 + 4k_h^2)^{1/2} \quad (10c)$$

Hence, substitution into Equation (9) permits one to express  $\chi_i$  via a single quadrature as (after introducing polar coordinates and integrating over the angle):

$$\chi_i(\mathbf{r}) = \begin{cases} \frac{S_0}{2} \int_0^\infty \frac{dk_h \tilde{\rho}(k_h) k_h^5}{\sqrt{1+(2k_h)^2}} \left[ \Theta\left(\frac{\rho_-}{2}\right) - \Theta\left(\frac{\rho_+}{2}\right) \right] J_0(r_h k_h) & i = 1 \\ \frac{S_0}{4} \int_0^\infty \frac{dk_h \tilde{\rho}(k_h) k_h^3}{\sqrt{1+(2k_h)^2}} \left[ \rho_+ \Theta\left(\frac{\rho_+}{2}\right) - \rho_- \Theta\left(\frac{\rho_-}{2}\right) \right] \left[ J_0(r_h k_h) - \frac{J_1(r_h k_h)}{r_h k_h} \right] & i = m \end{cases} \quad (11)$$

( $J_n$  denotes the n-order Bessel's function).

The second case is that of a medium with fully vertically correlated parameters. Such a model is appropriate to analyze flow and transport at regional scale [3]. Because in this case the Fourier transform  $\tilde{\rho}$  is

$$\tilde{\rho}(k) = \sqrt{2\pi}\tilde{\rho}_h(k_h)\delta(k_1) \tag{12}$$

( $\rho_h$  being the horizontal autocorrelation), it is easily proved from Equation (8) that

$$\chi_i(r_h) = \begin{cases} \lambda^{-1}\rho_h(r_h) & i = 1 \\ 0 & i = m \end{cases} \tag{13}$$

In line with past studies (e.g., [3]), Equation (13) clearly shows that assuming fully vertically correlated parameters implies that the formation may be sought as a bundle of noninteracting (i.e.,  $\chi_m = 0$ ) soil columns. Furthermore, it is also seen that the vertical flux autocorrelation decays like  $\lambda^{-1}$ .

Scaling  $k_1$  by the anisotropy ratio  $\lambda = \frac{L_v}{L}$  (for simplicity, we retain the same notation), the general expression (8) can be rewritten as

$$\chi_i(\mathbf{r}) = \begin{cases} \frac{\lambda^3}{(2\pi)^{3/2}} \int \frac{d\mathbf{k} \exp(-j\mathbf{k}\cdot\mathbf{r})\tilde{\rho}(k)(k^2-k_1^2)^2}{[k_1^2+\lambda^2(k^2-k_1^2)]^2+(\lambda k_1)^2} & i = 1 \\ \frac{\lambda}{(2\pi)^{3/2}} \int \frac{d\mathbf{k} \exp(-j\mathbf{k}\cdot\mathbf{r})\tilde{\rho}(k)(k_1 k_i)^2}{[k_1^2+\lambda^2(k^2-k_1^2)]^2+(\lambda k_1)^2} & i = m \end{cases} \tag{14}$$

The advantage of such a representation stems from the fact that  $\rho$  becomes isotropic, and therefore its Fourier transform will depend upon the modulus of  $\mathbf{k}$ , solely. As a consequence, we can further reduce the quadratures appearing into Equation (14) by adopting spherical coordinates and integrating over the azimuth angle, the result being:

$$\chi_i(r) = \begin{cases} \sqrt{\frac{2}{\pi}} \int_0^\infty \int_0^{1/\lambda} \frac{dk du k^4 \tilde{\rho}(k) \cos(\lambda r k u)}{u^2+k^2[1+(1-\lambda^2)u^2]^2} [1 - (\lambda u)^2]^2 & i = 1 \\ \frac{1}{\sqrt{2\pi}} \int_0^\infty \int_0^{1/\lambda} \frac{dk du k^4 \tilde{\rho}(k) \cos(\lambda r k u)}{u^2+k^2[1+(1-\lambda^2)u^2]^2} [1 - (\lambda u)^2] u^2 & i = m \end{cases} \tag{15}$$

The relationship (15) together with (7) provides a  $\sigma_\gamma^2$ -order representation of the flux covariance valid for arbitrary autocorrelation  $\rho$ .

In order to carry out the computation of (11), (13), and (15), we shall consider two types of models for  $\rho$ , namely the exponential and the Gaussian one. While the exponential model has been widely adopted (see, for instance, [20, 35, 36, 37]), there are very few studies (e.g., [30]) dealing with the Gaussian  $\rho$ . Nevertheless, many field findings (e.g., [1, 13, 17]) have shown that the

Gaussian model is also applicable. Before going on, it is worth emphasizing here that the general results (11), (13), and (15) are limited to the case of a flow normal to the formation bedding. The more general case of a flow arbitrary inclined with respect to the bedding was tackled by [25]. Finally, let us observe that the flux variance  $\sigma_{q_i}^2$  is obtained from Equation (7) as

$$\sigma_{q_i}^2 = \sigma^2 \exp(2\langle\Psi\rangle)\chi_i(0) \quad i = 1, 2, 3. \tag{16}$$

### 2.2 Results

We want to derive here explicit expressions for  $\chi_i$ . Thus, assuming exponential  $\rho$  permits us to carry out the quadrature over  $k$  into Equation (15) yielding:

$$\chi_1(r) = \int_0^{1/\lambda} du \bar{Y}(u, r) \left[ \frac{1 - u\zeta(u)}{1 - \zeta^2(u)} \right]^2 \quad \chi_m(r) = \int_0^{1/\lambda} du \bar{Y}(u, r) \frac{u\zeta(u)[1 - u\zeta(u)]}{2[1 - \zeta^2(u)]^2} \tag{17a}$$

$$\bar{Y}(u, r) = 2\zeta^3(u) \exp[\lambda ru\zeta(u)] + [1 - \lambda ru + (\lambda ru - 3)\zeta^2(u)] \exp(-\lambda ru) \tag{17b}$$

where we have set  $\zeta(t) = \frac{t}{1+(1-\lambda^2)t^2}$ . For an isotropic formation (i.e.,  $\lambda = 1$ ), we can express Equation (17a) in analytical form:

$$\chi_1(r) = [1 - (r + 1) \exp(-r)r^{-2}] \tag{18a}$$

$$\chi_m(r) = \frac{1}{2} \{ [E_i(-r) - E_i(-2r)] \exp(r) + (1 - \ln 2 + r^{-2}) \exp(-r) + (r - 1)r^{-2} \}. \tag{18b}$$

Instead, in the case of Gaussian  $\rho$ , the quadratures appearing into Equation (15) have to be numerically evaluated.

For  $r = 0$ , and dealing with small  $\lambda$ , we obtain

$$\chi_1(0) = \sqrt{\frac{\pi}{2}} \int_0^\infty \frac{dk \tilde{\rho}(k) k^3}{\sqrt{1 + (2k)^2}} \quad \chi_m(0) = \frac{\chi_1(0)}{2}. \tag{19}$$

In particular, assuming exponential structure for  $\rho$  yields  $\chi_1(0) = \frac{1}{3} (1 + \frac{2\pi}{9} \sqrt{3})$ , and for the Gaussian model one has  $\chi_1(0) = \frac{1}{4} \left[ 1 + (\pi - \frac{1}{2}) \exp(\frac{1}{4\pi}) \operatorname{erfc}(\frac{1}{2\sqrt{\pi}}) \right]$ .

In the case of an isotropic formation, it yields

$$\chi_1(0) = \frac{1}{2} \quad \chi_m(0) = \frac{3}{4} - \ln 2 \tag{20}$$

for exponential  $\rho$ , whereas for the Gaussian model one quadrature is required, the result being

$$\chi_1(0) = 0.504 \qquad \chi_m(0) = 0.060. \tag{21}$$

In the general case,  $\chi_i(0)$  are analytically computed for exponential autocorrelation:

$$\chi_1(0) = \frac{(2\lambda^2 - 1)(2\lambda - 1)}{(4\lambda^2 - 3)(\lambda^2 - 1)} + \frac{\ln(1 + \lambda)}{(\lambda^2 - 1)^2} + \frac{\text{sg}(1 - \lambda)(6\lambda^4 - 6\lambda^2 + 1)}{(4\lambda^2 - 3)\sqrt{|4\lambda^2 - 3|}(\lambda^2 - 1)^2} \tag{22a}$$

$$\chi_m(0) = -\frac{1}{2} \left[ \frac{2\lambda - 1}{(4\lambda^2 - 3)(\lambda^2 - 1)} + \frac{\ln(1 + \lambda)}{(\lambda^2 - 1)^2} + \frac{\text{sg}(1 - \lambda)(4\lambda^4 - 2\lambda^2 - 1)}{(4\lambda^2 - 3)\sqrt{|4\lambda^2 - 3|}(\lambda^2 - 1)^2} \right] \tag{22b}$$

with

$$\alpha(\lambda) = \begin{cases} 2 \left\{ \tan^{-1} \left[ \frac{P_2(\lambda)}{\lambda\sqrt{3-4\lambda^2}} \right] + \tan^{-1} \left( \frac{1}{\sqrt{3-4\lambda^2}} \right) \right\} & 3 \geq 4\lambda^2 \\ \ln \left\{ \left[ \frac{P_2(\lambda) + \text{sg}(\lambda-1)\lambda\sqrt{4\lambda^2-3}}{P_2(\lambda) - \text{sg}(\lambda-1)\lambda\sqrt{4\lambda^2-3}} \right] \left[ \frac{1 + \text{sg}(\lambda-1)\sqrt{4\lambda^2-3}}{1 - \text{sg}(\lambda-1)\sqrt{4\lambda^2-3}} \right] \right\} & 3 \leq 4\lambda^2 \end{cases}$$

being  $P_2(\lambda) = 2\lambda^2 - \lambda - 2$ , whereas  $\text{sg}(x)$  is the signum function.

For Gaussian  $\rho$ , we have (after integrating over  $k$ ):

$$\chi_1(0) = 2 \int_0^{1/\lambda} du [1 - u\zeta(u)]^2 \bar{\Phi}[\zeta(u)], \qquad \chi_m(0) = 2 \int_0^{1/\lambda} du u\zeta(u)[1 - u\zeta(u)] \bar{\Phi}[\zeta(u)] \tag{23a}$$

$$\bar{\Phi}(a) = \frac{1}{2} + \frac{a^2}{\pi} \left[ a \exp\left(\frac{a^2}{\pi}\right) \text{erfc}\left(\frac{a}{\sqrt{\pi}}\right) - 1 \right]. \tag{23b}$$

Observe that in the case of Equations (22a)–(22b), we can easily derive the following asymptotics:

$$\chi_1(0) = \frac{1}{3} \left( 1 + \frac{2\pi}{9} \sqrt{3} \right) + O(\lambda^2) \qquad \chi_m(0) = \frac{\chi_1(0)}{2} + O(\lambda^2) \qquad \lambda \ll 1 \tag{24a}$$

$$\chi_1(0) = O(\lambda^{-1}) \qquad \chi_m(0) = O(\lambda^{-3}) \qquad \lambda \gg 1. \tag{24b}$$

### 3 Macrodispersion Modelling

We want to use the above results concerning water flow to model macrodispersion. To do this, we briefly recall the Lagrangian description of a solute particle motion by random flows [31]. Thus, the displacement covariance  $\chi_{ii}(t)$  of a moving solute particle has been obtained by Dagan [4] as follows:



$$\chi_{ii}(t) = 2 \int_0^t d\tau(t - \tau)u_{ii}(\tau), \tag{25}$$

where  $u_{ii} = u_{ii}(t)$  represents the covariance of the pore velocity, this latter being defined as the ratio between the flux  $q$  and the effective water content  $\vartheta_e$  (i.e., the volumetric fraction of mobile water). The Fickian dispersion coefficients can be derived as asymptotic limit of the time-dependent dispersion coefficients  $D_{ii}$  (hereafter also termed *macrodispersion coefficients*) defined by

$$D_{ii}(t) = \frac{1}{2} \frac{d}{dt} X_{ii}(t) \tag{26}$$

[5]. To evaluate the covariance  $u_{ii}$ , in principle one should employ a second-order analysis similar to that which has led to Equation (7). However, field studies (e.g., [19, 26, 29]) as well as numerical simulations [21, 22] suggest that in uniform mean flows, the spatial variability of the effective water content may be neglected compared with the heterogeneity of the conductivity  $K$ . Thus, based on these grounds and similar to previous studies (e.g., [20, 24, 25]), we shall regard  $\vartheta_e$  as a constant uniformly distributed in the space, so that the pore velocity covariance is calculated as

$$u_{ii}(r) = \sigma^2 \exp(2\langle\Psi\rangle)\chi_i(r). \tag{27}$$

Inserting (27) into (25) provides the displacements covariance tensor

$$\frac{X_{ii}(t)}{l^2} = 2\sigma^2 \exp(2\langle\Psi\rangle) \int_0^t d\tau(t - \tau)\chi_i(\tau), \tag{28}$$

and concurrently the macrodispersion coefficients

$$\frac{D_{ii}(t)}{UI} = \sigma^2 \exp(2\langle\Psi\rangle) \int_0^t d\tau\chi_i(\tau). \tag{29}$$

Let's observe that the time has been scaled by  $\frac{l}{U}$  with  $U = \frac{K_0}{\vartheta_e}$  (even if we have kept the same notation). As it will be clearer later on, one important aspect related to Equation (29) is that the time dependency of  $D_{ii}$  is all encapsulated in the integral of the term  $\chi_i$ , which implies that (in the spirit of the assumptions underlying the current chapter) the rate of attainment of the Fickian regime is an intrinsic formation property. Furthermore, given the formation structure and for fixed mean pressure head, the enhanced solute spreading is due to an increase in the variance  $\sigma_\gamma^2$  in agreement with previous results (see [20, 21, 24]).

At the limit  $t \ll 1$ , the behaviour of  $\chi_i(t)$  and  $D_{ii}(t)$  is the general one resulting from the theory of [31], and it is

$$\frac{X_{ii}(t)}{I^2} = \sigma^2 \exp(2\langle\Psi\rangle)\chi_i(0)t^2 \quad \frac{D_{ii}(t)}{UI} = \sigma^2 \exp(2\langle\Psi\rangle)\chi_i(0)t. \quad (30)$$

The large time behaviour will be considered in the following.

## 4 Discussion

We want to quantify the impact of the relevant formation properties as well as mean pressure head upon the velocity spatial distribution and solute spreading. Before going on, we wish to identify here some practical values of the input parameters  $\sigma_\gamma^2$ .

Following the field studies of [19, 26, 29], we shall assume that  $Y$  and  $\zeta$  are independent RSFs, so that their cross-correlation can be ignored. The assumption of lack of correlation between  $Y$  and  $\zeta$  may be explained by the fact that  $Y$  is controlled by structural (macro) voids, whereas  $\zeta$  (or any other parameter related to the pore size distribution) is controlled by the soil texture [12].

The variance of  $\zeta$  can be either larger or smaller than that of  $Y$ . For example, [32] reported the  $\zeta$ -variance in the range 0.045–0.112 and the variance of  $Y$  in the range 0.391–0.960, whereas [26] found  $\sigma_\gamma^2 = 0.425$  compared with  $\sigma_\gamma^2 = 1.242$ . Instead, [34], and [19] found the variances of  $\zeta$  and  $Y$  to be of similar order, whereas [14, 15] observed the variance of  $\zeta$  to exceed that of  $Y$ . Thus, in what follows we shall allow  $\frac{\sigma_\zeta^2}{\sigma_Y^2}$  to vary between  $10^{-2}$  and 10 in order to cover a wide range of practical situations.

### 4.1 Velocity Analysis

In Fig. 1, the scaled velocity variances  $\frac{u_{ii}(0)}{(U\sigma)^2}\exp(-2\langle\Psi\rangle) = \chi_i(0)$  have been depicted versus the anisotropy ratio  $\lambda$ . Generally, the curves  $\chi_i(0)$  are monotonic decreasing approaching to zero for large  $\lambda$ . In particular,  $\chi_m(0)$  vanish faster than  $\chi_1(0)$  in accordance with Equation (13). At small  $\lambda$ , the curves  $\chi_i(0)$  assume the constant values (20)–(21). From Fig. 1, it is also seen that  $\chi_m(0) < \chi_1(0)$ . The physical interpretation of this is that fluid particles can circumvent inclusions of low conductivity laterally in two directions, causing them to depart from the mean trajectory to a lesser extent than in the longitudinal direction. Moreover, assuming different shapes of  $\rho$  does not significantly impact  $\chi_i(0)$ . Finally, it is worth observing that the  $\chi_i(0)$  curves calculated for the exponential model lead to the same expression of the flux variances obtained by [36].

To grasp the combined effect of the medium heterogeneity and the mean pressure head upon the velocity variance, we have depicted in Fig. 2 the contour lines of the ratio  $\frac{u_{ii}(0)}{\chi_i(0)(U\sigma_\gamma)^2} = \Lambda$ .

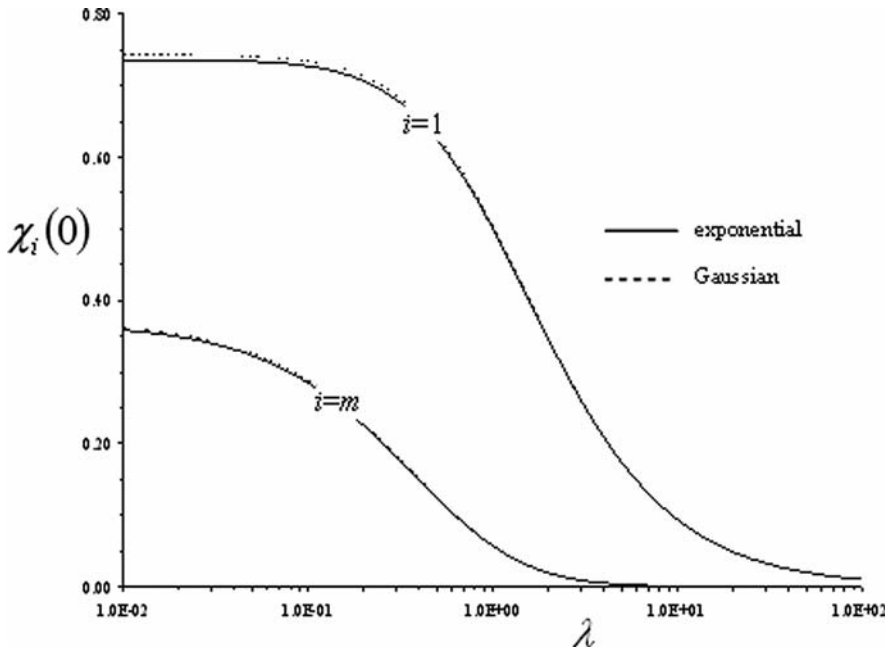


Fig. 1 Dependence of the scaled variances  $\chi_i(0)$  for both the exponential (solid line) and the Gaussian model (dashed line) upon the anisotropy ratio  $\lambda$

The  $\Lambda$ -function decreases when (i) the variability of the capillary forces reduces compared with that of the saturated conductivity (for fixed  $\langle\Psi\rangle$ ) and (ii) the porous formation becomes drier in mean (for given  $\frac{\sigma_x^2}{\sigma_y^2}$ ). This last result is due to the fact that an increase of suction reduces *de facto* the fluid particles mobility. For  $\sigma_\zeta^2 < \frac{\sigma_x^2}{10}$ , the isolines are practically vertical suggesting that in this case, the velocity variance is mainly influenced by the mean flow conditions. To the contrary, for  $\sigma_\zeta^2 > \sigma_y^2$ , the isolines tend to become horizontal implying that the flow conditions have a negligible effect upon  $\Lambda$ .

The relationship (7) shows that the contributions of the mean flow combined with the variance of the input parameters and the domain structure are separated into a multiplicative form. As a consequence, the velocity autocorrelation

$$\rho_{u_i}(r) = \frac{C_{u_i}(r)}{C_{u_i}(0)} = \frac{\chi_i(r)}{\chi_i(0)} \tag{31}$$

is a formation property, and therefore it is applicable to both saturated and unsaturated porous media. This is demonstrated by the good agreement (Fig. 3a, b) between (31) calculated for the exponential  $\rho$  (solid line) and the velocity autocorrelation (symbols) (obtained by [23]) for the same model of  $\rho$ ,

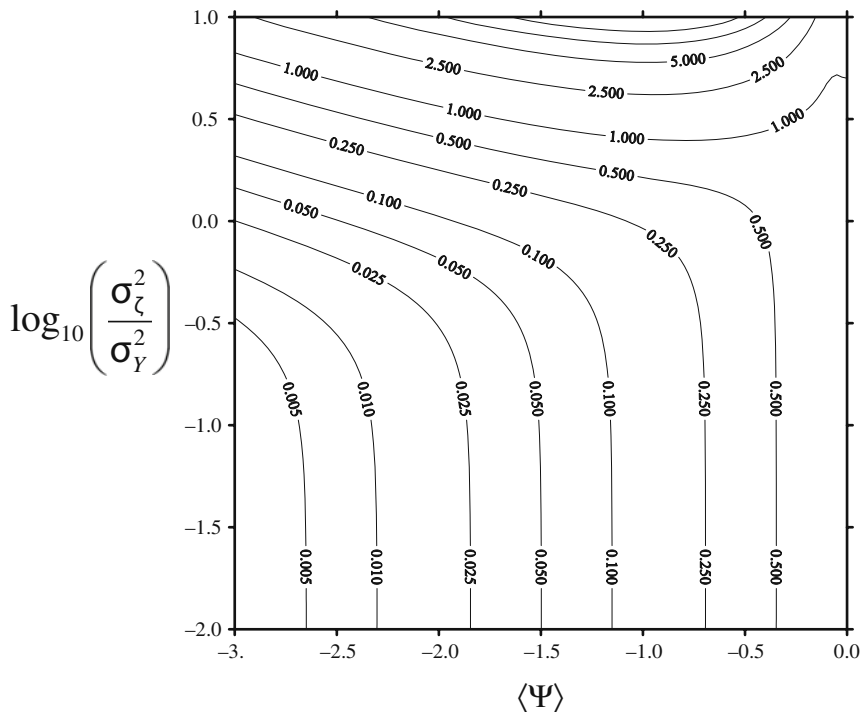


**Fig. 2** Contour lines of  $\Lambda$  versus the scaled mean pressure head  $\langle \Psi \rangle$ , and the ratio  $\sigma_z^2 / \sigma_y^2$

and dealing with a mean groundwater flow normal to the formation bedding (Equations (15a)–(15b) in [23]). Such a result was anticipated by Russo [24], who used the velocity covariance obtained for saturated flow conditions to analyze transport in a vadose zone.

For completeness, in Fig. 3a, b we have also reported the velocity autocorrelation (dashed line) corresponding with the Gaussian model of  $\rho$ . At a first glance, it is seen that the shape of  $\rho$  plays an important role in determining the behaviour of the velocity correlation. More precisely, close to the origin the autocorrelation  $\rho_{ii}$ , evaluated via the exponential  $\rho$  decays faster than that obtained by adopting the Gaussian model, whereas the opposite is observed at large  $r$ . This is due to the faster vanishing with distance of the Gaussian model compared with the exponential one. Similar results were obtained by other authors (for a wide review, see [38]).

The dependence of the velocity autocorrelation (Fig. 3a, b) upon the anisotropy ratio  $\lambda$  can be explained as follows: as water moves in the porous medium, a low conductivity inclusion (say a flow barrier) occurs that makes the velocity covariance decay with the separation distance. The possibility to circumvent a flow barrier will drastically decrease, and concurrently the distance over which the velocity is correlated will increase, as the typical horizontal size of the flow barrier is prevailing upon the vertical one, and vice versa. This justifies the

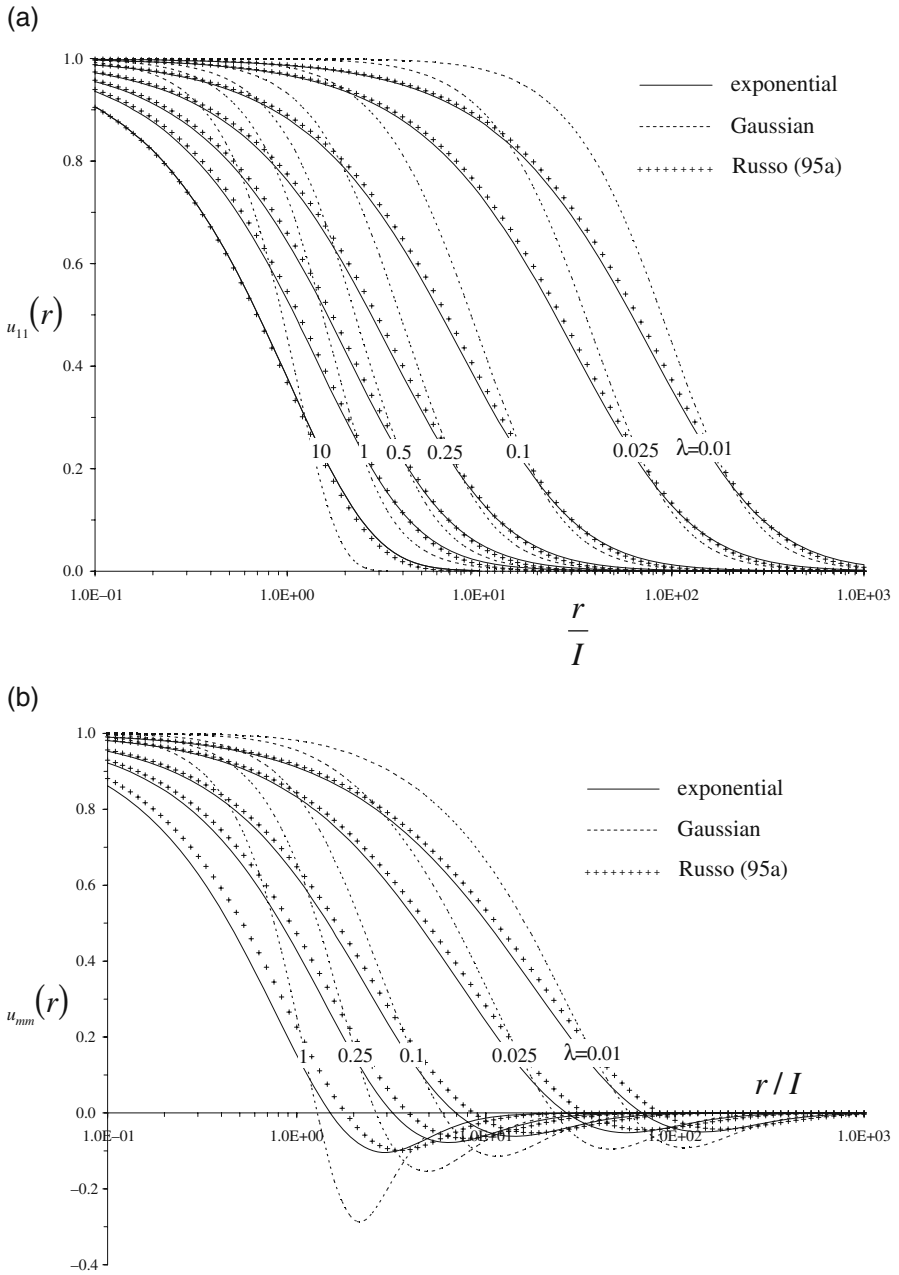


**Fig. 3** (a) Longitudinal and (b) transversal components of the autocorrelation velocity versus the dimensionless distance ( $r/I$ ) for various values of the anisotropy ratio  $\lambda$

persistence of the velocity correlation at small  $\lambda$ , whereas it rapidly decays at high anisotropic ratios attaining the limiting case (13) practically for  $\lambda \geq 10$ .

Finally, it is worth observing here that basic results concerning the structure of the velocity autocorrelation are of general validity (in the spirit of the assumptions we have adopted), and therefore they are not limited to a vadose zone exhibiting zero cross-correlation between  $Y$  and  $\zeta$ .

### 4.2 Spreading Analysis

Once the velocity covariance is calculated, the components of the displacement covariance tensor  $\chi_{ii}$  are evaluated by the aid of Equation (28). In the early time regime, the  $\chi_{ii}$  components are characterized by the quadratic time dependence (although the displacement tensor is anisotropic) according to Equation (30). As a consequence, at this stage the relative dispersion  $\frac{\chi_{nm}}{\chi_{11}}$  will result equal to  $\frac{\chi_{nm}(0)}{\chi_{11}(0)}$ , and therefore it results in a formation property. This is clearly seen in Fig. 4, where we have compared  $\frac{\chi_{nm}(0)}{\chi_{11}(0)}$  with the same quantity calculated when considering a mean groundwater flow normal to the formation bedding [23]. In the same figure, it also seen that  $\frac{\chi_{nm}}{\chi_{11}}$  is a monotonic decreasing function of the anisotropic ratio  $\lambda$ . This is due to the fact that as  $\lambda$  increases, the tortuosity of lateral paths reduces compared with that along the longitudinal direction. As

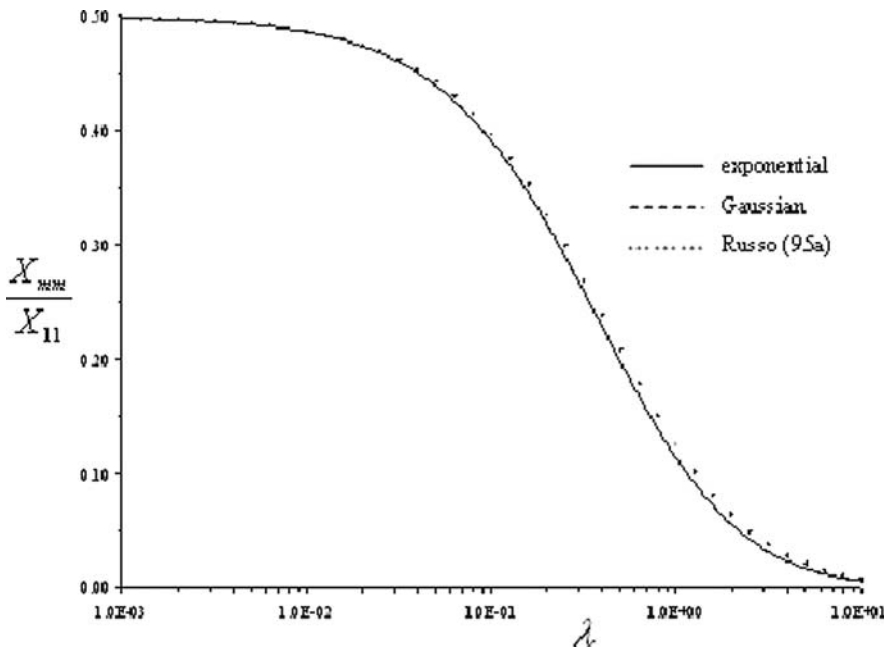


Fig. 4 Dependence of the early time relative dispersion  $X_{nm}/X_{11}$  upon the anisotropy ratio  $\lambda$

expected from Equation (19), at small anisotropic ratios (say for  $\lambda < 0.01$ ),  $\frac{X_{mm}}{\chi_{11}}$  is equal to  $\frac{1}{2}$  irrespective of  $\rho$ . At any rate, even at higher  $\lambda$ , the shape of  $\rho$  is found practically immaterial.

By considering exponential  $\rho$ , the computation of  $\chi_{ii}(t)$  is reduced to one integral solely:

$$X_{11}(t) = 2 \left( \frac{I\sigma}{\lambda} \right)^2 \exp(2\langle\Psi\rangle) \int_0^{1/\lambda} du \bar{\Gamma}(u, t) \left\{ \frac{1 - u\zeta(u)}{u[1 - u\zeta^2(u)]} \right\}^2 \tag{32a}$$

$$X_{mm}(t) = \left( \frac{I\sigma}{\lambda} \right)^2 \exp(2\langle\Psi\rangle) \int_0^{1/\lambda} du \bar{\Gamma}(u, t) \frac{\zeta(u)}{u} \frac{[1 - u\zeta(u)]}{[1 - u\zeta^2(u)]^2} \tag{32b}$$

$$\bar{\Gamma}(u, t) = 2\zeta(u) \exp[-\lambda u\zeta(u)t] + [(\lambda ut - 1)\zeta^2(u) - (\lambda ut + 1)] \exp(-\lambda ut) + [\zeta(u) - 1]^2. \tag{33}$$

Like groundwater flow [5], for an isotropic formation we can express (32a)–(32b) in analytical form, that is,

$$X_{11}(t) = 2(I\sigma)^2 \exp(2\langle\Psi\rangle) \{t - [\ln t - E_i(-t) + E]\} \tag{34a}$$

$$X_{mm}(t) = (I\sigma)^2 \exp(2\langle\Psi\rangle) \{[E_i(-t) - E_i(-2t)] \exp(t) - (\ln 2 - 1) \exp(-t) + 2 \ln 2 - 1\} \tag{34b}$$

( $E$  represents the constant of Euler–Mascheroni).

The dependence of the scaled longitudinal covariance  $\frac{X_{11}(t)}{(I\sigma)^2} \exp(-2\langle\Psi\rangle) = \bar{X}_{11}(t)$  upon the time and for several values of the anisotropic ratio has been depicted in Fig. 5. As the solute body invades the flow system,  $\bar{X}_{11}$  grows monotonically with the time. The early as well as large time regime are those predicted by the theory of Taylor [31], that is, a nonlinear time dependence (whose persistence increases as the anisotropic ratio reduces) on short times, whereas for  $t$  large enough,  $\bar{X}_{11}$  grows linearly with time. Regarding the dependence of  $\bar{X}_{11}(t)$  upon the anisotropy ratio, preliminary simulations have shown that for  $\lambda \leq 0.01$ , the longitudinal covariance components can be evaluated by adopting Equation (11) for  $\chi_1(\tau)$ . Instead, for  $\lambda > 10$ , we obtain from (13) and (28)–(29) the following results:

$$\frac{X_{11}(t)}{I^2} = \frac{2\sigma^2}{\lambda} \exp(2\langle\Psi\rangle) \Xi(t) \qquad \frac{D_{11}(t)}{UI} = \frac{\sigma^2}{\lambda} \exp(2\langle\Psi\rangle) \Delta(t) \tag{35}$$

with

$$\Xi(t) = t + \rho_h(t) - 1 \qquad \Delta(t) = 1 - \rho_h(t) \tag{36}$$

for exponential  $\rho_h$ , whereas

$$\Xi(t) = t \operatorname{erf}(\sqrt{\pi}t) + \frac{2}{\pi} [\rho_h(t) - 1] \qquad \Delta(t) = \operatorname{erf}(\sqrt{\pi}t) \tag{37}$$

for Gaussian  $\rho_h$ .

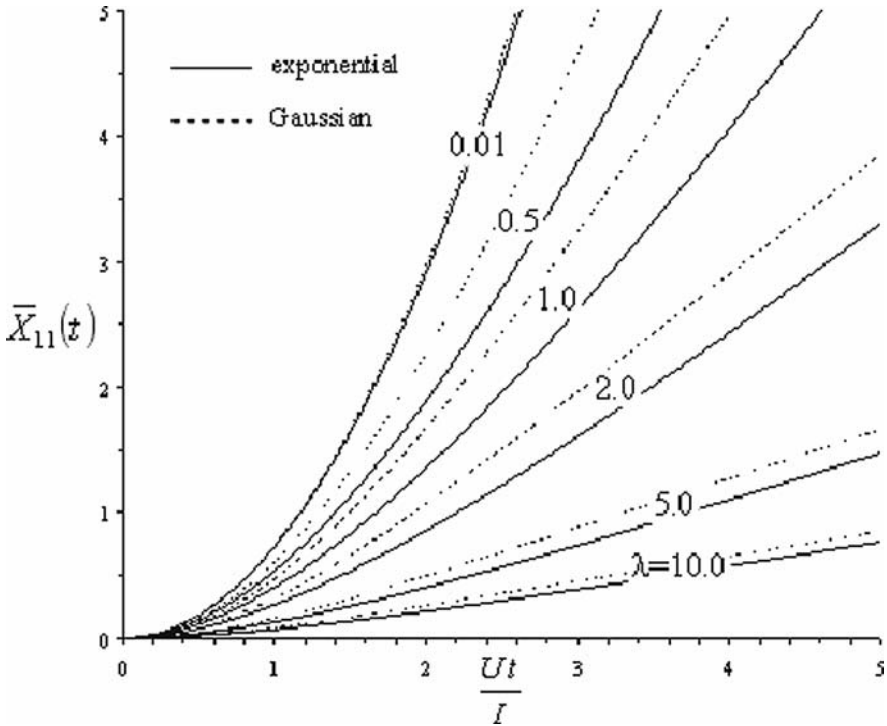


**Fig. 5** Longitudinal component of the time-dependent scaled displacement covariance tensor  $\bar{X}_{11}(t)$  for different values of the anisotropy ratio  $\lambda$

The behaviour of the transverse components in the early time regime is similar to  $X_{11}$  in the sense that  $\frac{X_{mm}(t)}{(\sigma)^2} \exp(-2\langle\Psi\rangle) = \bar{X}_{mm}(t)$  increases with the travel time at a faster rate than linearly. However, unlike the longitudinal components,  $X_{mm}$  approach constant asymptotic values as the solute body moves (see also [20]). In particular, for exponential  $\rho$ , integration of Equation (32b) with respect to  $u$  is carried out after taking the limit  $t \rightarrow \infty$  to yield

$$X_{mm}(\infty) = \frac{sg(4\lambda^2 - 3)}{\lambda^2|4\lambda^2 - 3|^{3/2}} \left[ (1 - 2\lambda)\sqrt{|4\lambda^2 - 3|} + 2(2\lambda^2 - 1)\beta(\lambda) \right] \quad (38a)$$

$$\beta(\lambda) = \begin{cases} 2 \arctan\left(\frac{\sqrt{3-4\lambda^2}}{1+2\lambda}\right) & 4\lambda^2 \leq 3 \\ \ln\left\{ \frac{P_2(\lambda)+\lambda\sqrt{4\lambda^2-3}}{P_2(\lambda)-\lambda\sqrt{4\lambda^2-3}} \left( \frac{1+\sqrt{4\lambda^2-3}}{1-\sqrt{4\lambda^2-3}} \right) \right\} & 4\lambda^2 \geq 3. \end{cases} \quad (38b)$$



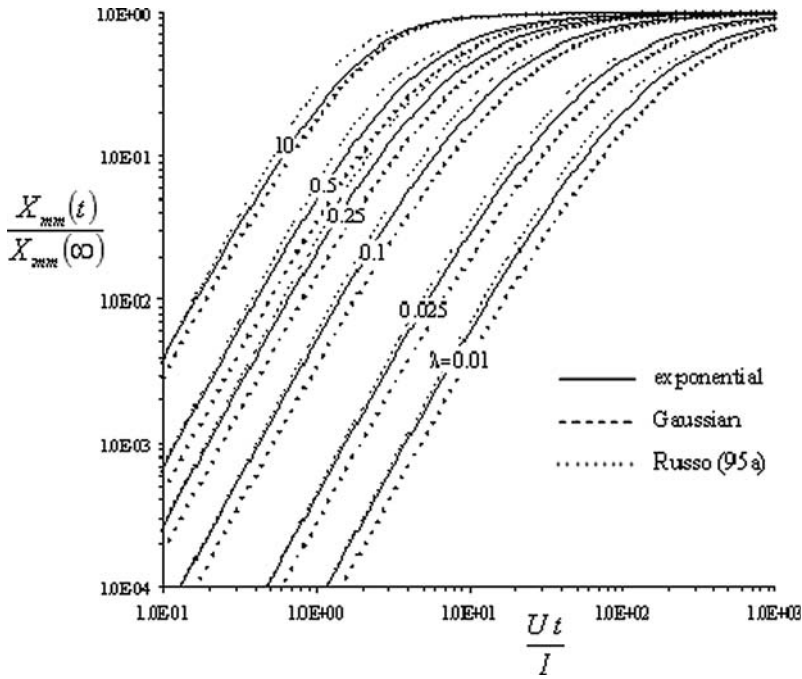


Fig. 6 Lateral component of the time-dependent scaled displacement covariance tensor  $X_{mmm}(t)/X_{mmm}(\infty)$  for different values of the anisotropy ratio  $\lambda$

To illustrate the impact of the formation anisotropy on the rate at which  $X_{mmm}(t)$  approach their asymptotic values, we have depicted in Fig. 6 the normalized transverse variance  $\frac{X_{mmm}(t)}{X_{mmm}(\infty)}$  for both the exponential (solid line) and the Gaussian model (dashed line) versus the time, and for different values of  $\lambda$ .

At given time, as  $\lambda$  decreases, the ratio  $\frac{X_{mmm}(t)}{X_{mmm}(\infty)}$  reduces, and vice versa. In fact, a large  $\lambda$  means that any low conductivity inclusion is less than an obstruction to the vertical flow, as streamlines can easily bypass it laterally, thus reducing the transverse spread. This enables the solute particles to approach the Fickian regime faster. Similarly to the previous section, a fundamental consequence of the separation structure of Equation (28) is that the distance needed to reach Fickian conditions is an intrinsic formation property. To show this, we have depicted in Fig. 6 the ratio (symbols) between the transverse displacement covariance and their asymptotic values as calculated from equations (21b) and (23) reported in [23], which are valid for groundwater flow normal to the formation bedding.

The macrodispersion coefficients are calculated in a straightforward manner by combining the general result (29) with the above-derived displacement covariance tensor. Thus, for  $\rho = \exp(-r)$ , we can express  $D_{ii}$  in terms of one quadrature solely:

$$\frac{D_{11}(t)}{UI} = \frac{\sigma^2}{\lambda} \exp(2\langle\Psi\rangle) \int_0^{1/\lambda} du \frac{\bar{\Gamma}(u, t)}{u} \left\{ \frac{1 - u\zeta(u)}{u[1 - \zeta^2(u)]} \right\}^2 \quad (39a)$$

$$\frac{D_{mm}(t)}{UI} = \frac{\sigma^2}{2\lambda} \exp(2\langle\Psi\rangle) \int_0^{1/\lambda} du \bar{\Gamma}(u, t) \frac{\zeta(u)[1 - u\zeta(u)]}{[1 - \zeta^2(u)]^2} \quad (39b)$$

$$\bar{\Gamma}(u, t) = [\lambda ut + (2 - \lambda ut)\zeta^2(u)] \exp(-\lambda ut) - 2\zeta^2(u) \exp[-\lambda u\zeta(u)t] \quad (40)$$

In particular, for isotropic formations (39a)–(39b), provide closed form solutions, that is,

$$\frac{D_{11}(t)}{UI} = \sigma^2 \exp(2\langle\Psi\rangle) \frac{\exp(-t) + t - 1}{t} \quad (41)$$

$$\frac{D_{mm}(t)}{UI} = \sigma^2 \exp(2\langle\Psi\rangle) \frac{t[E_i(-t) - E_i(-2t)] \exp(t) + [t \ln 2 - (t + 1)] \exp(-t) + 1}{2t}. \quad (42)$$

Because the longitudinal covariance  $X_{11}$  grows linearly after travelling a certain distance, the longitudinal macrodispersivity is expected to become constant at this limit. Indeed, we have depicted in Fig. 7 the dimensionless longitudinal

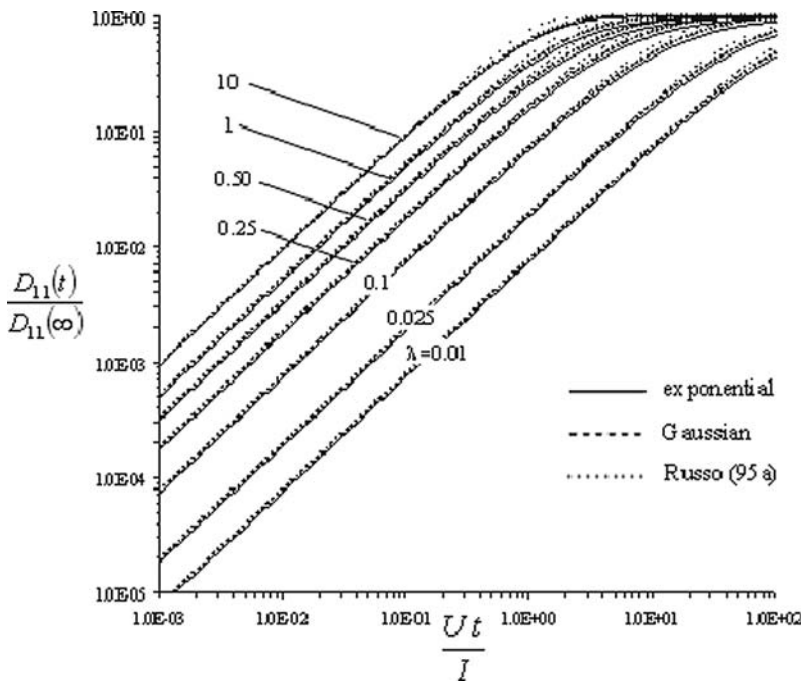


Fig. 7 Longitudinal scaled macrodispersion coefficient  $D_{11}(t)/D_{11}(\infty)$  as function of the dimensionless time  $Ut/I$  and for different values of the anisotropy ratio  $\lambda$

macrodispersion coefficient  $\frac{D_{11}(t)}{D_{11}(\infty)}$  versus the time for few values of the anisotropy ratio. The curves are plotted by considering the exponential as well as Gaussian model for  $\rho$ . The lower  $\lambda$  is, the larger is the distance the solute body has to traverse in order to get its asymptotic regime. This is because low values of  $\lambda$  require the solute plume to travel a longer distance to fully sample the formation heterogeneity and therefore to reach the Fickian regime. In the same figure, we have also depicted the same ratio  $\frac{D_{11}(t)}{D_{11}(\infty)}$  calculated for groundwater flow normal to the bedding (see [23]) to emphasize the intrinsic character of the distance needed to reach the asymptotic regime.

The transverse components of the macrodispersion tensor tend to zero at large  $t$ . This is a direct consequence of the fact that at this limit,  $X_{mm}$  tend to a finite value (see Fig. 6). Nevertheless, the magnitude of the transverse macrodispersion coefficients is deeply influenced by the formation anisotropy. Indeed, in Fig. 8 we have reported the quantity  $\frac{D_{mm}(t)}{U\Gamma\sigma^2} \exp(-2\langle\Psi\rangle)$  as a function of time. After an initial growth faster than linearly in  $t$ ,  $D_{mm}$  drops to zero more slowly as  $\lambda$  decreases (in line with the physical interpretation given to explain the behaviour of  $X_{mm}$ ). Finally, let's observe that the lateral dispersion is higher for Gaussian  $\rho$  at early times, whereas the opposite is seen asymptotically. This

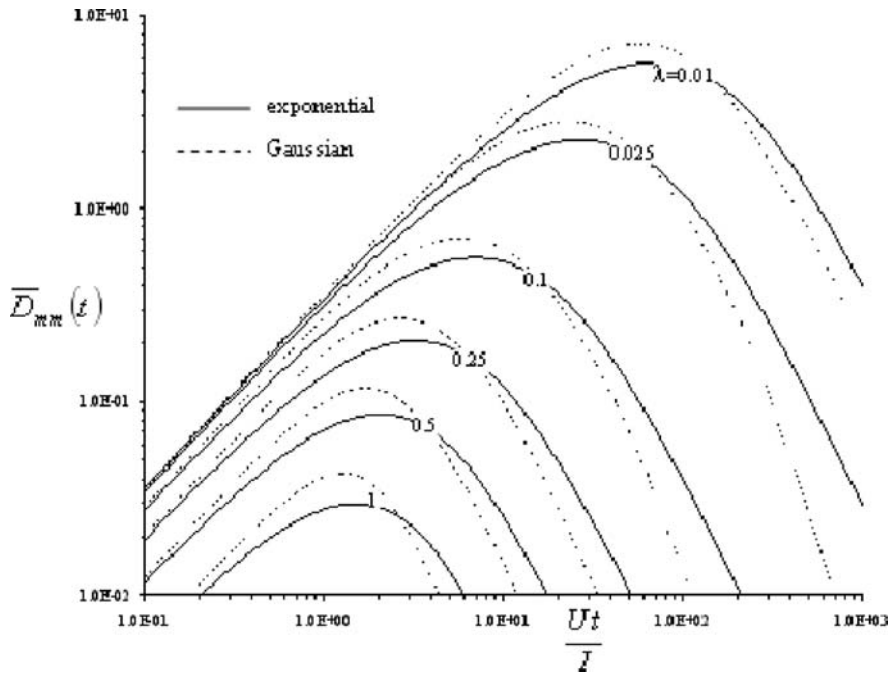


Fig. 8 Time dependence of the scaled lateral macrodispersion coefficients  $\bar{D}_{mm}(t)$  for different values of the anisotropy ratio  $\lambda$

is a consequence of the fact that at small arguments (see Fig. 3b), the Gaussian function causes a longer persistence of the correlation compared with the exponential model, whereas the opposite is observed at higher arguments.

## 5 Conclusions

The basic aim of the current chapter has been to analyze flow velocity and solute spreading in partially saturated heterogeneous porous formations by means of analytical tools. We have obtained simple results that permit one to grasp the main features of transport phenomena taking place in a vadose zone. This has been accomplished by combining the general Lagrangian formulation developed in the past (e.g., [5, 20]), and relating the spatial moments of a moving solute body to the velocity field, with the analytical results of [30] concerning steady unsaturated flow in an unbounded domain.

One of the main findings is the representation (27) of the velocity covariance. It is expressed by means of two quadratures, and it is valid for arbitrary (cross)correlation functions. In addition, simple results are derived by dealing with highly vertically anisotropic formations (i.e.,  $\lambda < 1$ ), and with the case of  $\lambda \gg 1$ . It is demonstrated that the velocity autocorrelation is an intrinsic formation property, and therefore it is applicable to both saturated and unsaturated porous media. As a consequence, the rate of approaching the asymptotic (Fickian) regime is also a formation property.

The velocity autocorrelation is characterized by finite correlation scales in accordance with previous studies (e.g., [20]). The rate of correlation decay is slower for vertically anisotropic formations, and it approaches to the limit case of highly vertically anisotropic formation for  $\lambda < 0.01$ . For larger  $\lambda$ , the velocity autocorrelation exhibits a much faster decay with the distance, and it approaches (say for  $\lambda > 10$ ) to that which we obtain when considering a medium with fully vertically correlated parameters. Also, the shape of the autocorrelation function of the input parameters is important in determining the behaviour of the spatial distribution of the velocity correlation. Indeed, for a Gaussian model, the persistence of the correlation is longer at small relative distances compared with that observed by adopting exponential  $\rho$ . The opposite is seen at large distances. This explains the basic differences between the components of the particle displacement covariance tensor.

For given variance of the input parameters and mean pressure head, the velocity variances are monotonic decreasing functions of the anisotropy ratio. In particular, the transverse velocity variance is smaller than the longitudinal one as fluid particles can bypass more easily any perturbation in the conductivity field in the transverse directions. Conversely, given the anisotropy structure of the formation, the magnitude of the velocity variance increases as the soil becomes more saturated, and it is enhanced when the variability of the saturated conductivity is small compared with that of the capillary forces.

The dimensionless  $\frac{\chi_{ii}(t)}{(I_0)^2} \exp(-2\langle\Psi\rangle)$  components of the displacement covariance tensor are in agreement with the general Lagrangian results concerning flow in random fields (see [5, 23, 24]). An increase of suction reduces the fluid particles mobility, and therefore the magnitude of the displacements covariance. In the case of exponential model for  $\rho$ , analytical closed forms are derived for  $\chi_{mm}$  in the asymptotic regime. The behaviour of the macrodispersion coefficients  $D_{ii}(t)$  reflects that of the covariance displacements. Thus,  $D_{11}(t)$  asymptotically tends to the constant (Fickian) value  $D_{11}(\infty)$ . The rate of approaching to  $D_{11}(\infty)$  is an intrinsic formation property. It is also shown that the transverse macrodispersion coefficients  $D_{mm}(t)$  asymptotically tend to zero with a rate that is faster for Gaussian  $\rho$ .

We would like to emphasize that the current analysis of water flow and solute transport in a vadose zone is based on a small-perturbation analysis following the linear theory of Dagan [4]. It is generally accepted [5] that under saturated conditions, the linear theory captures the foremost features of transport phenomena whenever the variability of the saturated hydraulic conductivity is small (i.e.,  $\sigma_Y^2 \ll 1$ ). However, numerical simulations [2] as well as theoretical studies [6] on transport under steady groundwater flow show a broader range of applicability (say  $\sigma_Y^2 \approx 1$ ) because of the mutual cancellation effects of the errors induced by the linearization procedure. In the case of unsaturated flow, the nonlinear effects are expected to be larger because of the larger variability of the random input parameters [20]. However, because we have shown that the structure of the velocity autocorrelation is an intrinsic formation property, it is reasonable to expect that even for the unsaturated flow, the linear theory is applicable under a relatively wide range of practical situations. This has been tested numerically by Russo [18].

Finally, we want to underline that although the Fickian regime attainment is an intrinsic medium property, it is worth recalling that such a result relies on the assumptions underling the current study. Hence, it should not be employed in situations (like unsaturated flow close to the groundwater table or when accounting for the water content variability) that are not in compliance with such assumptions.

**Acknowledgments** The authors express sincere thanks to Dr. Gabriella Romagnoli for reviewing the manuscript. This study was supported by the grant PRIN (# 2004074597).

## References

1. Byers, E., and Stephans, D., B., 1983, Statistical and stochastic analyses of hydraulic conductivity and particle-size in fluvial sand, *Soil Sci. Soc. Am. J.*, 47, 1072–1081.
2. Chin, D., A. and Wang, T., 1992, An investigation of the validity of first-order stochastic dispersion theories in isotropic porous media, *Water Resour. Res.*, 28, 1531–1542.
3. Dagan, G., and Bresler, E., 1979, Solute dispersion in unsaturated heterogeneous soil at field scale: theory, *Soil Sci. Soc. Am. J.*, 43, 461–467.

4. Dagan, G., 1984, Solute transport in heterogeneous porous formations, *J. Fluid Mech.*, 145, 151–177.
5. Dagan, G., 1989, *Flow and Transport in Porous Formations*, Springer.
6. Dagan, G., Fiori, A., and Janković, I., 2003, Flow and transport in highly heterogeneous formations: I. Conceptual framework and validity of first-order approximations, *Water Resour. Res.*, 39, 1268, doi: 10.1029/2002WR001717.
7. Fiori, A., Indelman, P. and Dagan, G., 1998, Correlation structure of flow variables for steady flow toward a well with application to highly anisotropic heterogeneous formations, *Water Resour. Res.*, 34, 699–708.
8. Gardner, W., R., 1958, Some steady state solutions of unsaturated moisture flow equations with application to evaporation from a water table, *Soil Sci.*, 85, 228–232.
9. Gelhar, L., W., 1993, *Stochastic Subsurface Hydrology*, Prentice Hall.
10. Harter, Th., and Zhang, D., 1999, Water flow and solute spreading in heterogeneous soils with spatially variable water content, *Water Resour. Res.*, 35, 415–426.
11. Indelman, P., Or, D. and Rubin, Y., 1993, Stochastic analysis of unsaturated steady state flow through bounded heterogeneous formations, *Water Resour. Res.*, 29, 1141–1147.
12. Jury, W., A., Russo, D., and Sposito, G., 1987, The spatial variability of water and solute transport properties in unsaturated soil, II. Analysis of scaling theory, *Hilgardia*, 55, 33–57.
13. Nielsen, D., R., Biggar, J., W., and Erh, K., T., 1973, Spatial variability of field measured soil-water properties, *Hilgardia*, 42, 215–259.
14. Ragab, R., and Cooper, J., D., 1993a, Variability of unsaturated zone water transport parameters: implications for hydrological modelling, 1. In-situ measurements, *J. Hydrol.*, 148, 109–131.
15. Ragab, R., and Cooper, J., D., 1993b, Variability of unsaturated zone water transport parameters: implications for hydrological modelling, 2. Predicted vs. in-situ measurements and evaluation methods, *J. Hydrol.*, 148, 133–147.
16. Reynolds, W., D., and Elrick, D., E., 1985, In-situ measurement of field-saturated hydraulic conductivity, sorptivity, and the  $\alpha$ -parameter using the Guelph permeameter, *Soil Sci.*, 140, 292–302.
17. Russo, D., and Bresler, E., 1981, Soil hydraulic properties as stochastic processes, 1, Analysis of field spatial variability, *Soil Sci. Soc. Am. J.*, 45, 682–687.
18. Russo, D., 1988, Determining soil hydraulic properties by parameter estimation: on the selection of a model for the hydraulic properties, *Water Resour. Res.*, 24, 453–459.
19. Russo, D. and Bouton, M., 1992, Statistical analysis of spatial variability in unsaturated flow parameters, *Water Resour. Res.*, 28, 1911–1925.
20. Russo, D., 1993, Stochastic modeling of macrodispersion for solute transport in a heterogeneous unsaturated porous formation, *Water Resour. Res.*, 29, 383–397.
21. Russo, D., Zaidel, J., and Laufer, A., 1994a, Stochastic analysis of solute transport in partially saturated heterogeneous soils: I. Numerical experiments, *Water Resour. Res.*, 30, 769–779.
22. Russo, D., Zaidel, J., and Laufer, A., 1994b, Stochastic analysis of solute transport in partially saturated heterogeneous soils: II. Prediction of solute spread and breakthrough, *Water Resour. Res.*, 30, 781–790.
23. Russo, D., 1995a, On the velocity covariance and transport modeling in heterogeneous anisotropic porous formations 1. Saturated flow, *Water Resour. Res.*, 31, 129–137.
24. Russo, D., 1995b, On the velocity covariance and transport modeling in heterogeneous anisotropic porous formations 2. Unsaturated flow, *Water Resour. Res.*, 31, 139–145.
25. Russo, D., 1995c, Stochastic analysis of the velocity covariance and the displacement covariance tensors in partially saturated heterogeneous anisotropic porous formations, *Water Resour. Res.*, 31, 1647–1658.
26. Russo, D., Russo, I., and Laufer, A., 1997, On the spatial variability of parameters of the unsaturated hydraulic conductivity, *Water Resour. Res.*, 33, 947–956.

27. Russo, D., 1998, Stochastic analysis of flow and transport in unsaturated heterogeneous porous formations: effects of variability in water saturation, *Water Resour. Res.*, 34, 569–581.
28. Russo D., 2002, Stochastic analysis of macrodispersion in gravity-dominated flow through bimodal heterogeneous unsaturated formations, *Water Resour. Res.*, 38, 1114, doi: 10.1029/2001WR000850.
29. Severino, G., Santini, A., and Sommella, A., 2003, Determining the soil hydraulic conductivity by means of a field scale internal drainage, *J. Hydrol.*, 273, 234–248.
30. Severino, G., and Santini, A., 2005, On the effective hydraulic conductivity in mean vertical unsaturated steady flows, *Adv. Water Resour.*, 28, 964–974.
31. Taylor, G., I., 1921, Diffusion by continuous movements, *Proc. Lond. Math. Soc.*, A20, 196–211.
32. Ünlü, K., Nielsen, D., R., Biggar, J., W., and Morkoc, F., 1990, Statistical parameters characterizing the spatial variability of selected soil hydraulic properties, *Soil Sci. Soc. Am. J.*, 54, 1537–1547.
33. White, I., and Sully, M. J., 1987, Macroscopic and microscopic capillary length and time scales from field infiltration, *Water Resour. Res.*, 23, 1514–1522.
34. White, I., and Sully, M., J., 1992, On the variability and use of the hydraulic conductivity alpha parameter in stochastic treatment of unsaturated flow, *Water Resour. Res.*, 28, 209–213.
35. Yeh, T-C, J., Gelhar, L., W., and Gutjahr, A., 1985a, Stochastic analysis of unsaturated flow in heterogenous soils 1. Statistically isotropic media, *Water Resour. Res.*, 21, 447–456.
36. Yeh, T-C, J., Gelhar, L., W., and Gutjahr, A., 1985b, Stochastic analysis of unsaturated flow in heterogenous soils 2. Statistically anisotropic media with variable  $\alpha$ , *Water Resour. Res.*, 21, 457–464.
37. Zhang, D., Wallstrom, T., C., and Winter, C., L., 1998, Stochastic analysis of steady-state unsaturated flow in heterogeneous media: comparison of the Brooks-Corey and Gardner-Russo models, *Water Resour. Res.*, 34, 1437–1449.
38. Zhang, D., 2002, *Stochastic Methods for Flow in Porous Media*, Academic Press.